Brazilian Journal of Physics (2021) 51:958–968
https://doi.org/10.1007/s13538-021-00910-x

SOCIEDADE BRASILEIRA DE FÍSICA

ATOMIC PHYSICS

DFT Study of Conformational Analysis, Molecular Structure and Properties of *para*-, *meta*- and *ortho* 4-Methoxyphenyl Piperazine Isomers

Yavuz Ekincioğlu[1] · **Hamdi Şükür Kılıç**[1,2,3] · **Ömer Dereli**[4]

Received: 28 December 2020 / Accepted: 14 April 2021 / Published online: 26 April 2021

Abstract
In this study, conformer analysis of isomer structures of *para*-, *meta*- and *ortho* 4-methoxyphenyl piperazine molecules was performed using the Spartan 08 package program. The optimized geometrical parameters, energies for the highest occupied molecular orbital and the lowest unoccupied molecular orbitals, chemical reactivity descriptors, nonlinear optical properties, Mulliken population analysis, molecular electrostatic potential map, thermodynamic properties and UV–Vis spectral analysis of isomers of the N-(4-methoxyphenyl) piperazine molecule were predicted using the density functional theory (DFT) and TD-DFT/B3LYP/6-311++G(d,p) methods. The theoretical results obtained were compared with experimental results available in the literature so far, and these results were discussed for each isomer.

Keywords Methoxyphenyl piperazine · DFT · TD-DFT · NLO · UV–Vis

1 Introduction

Piperazine and its derivatives exist in many drug structures such as antipsychotic, antidepressant and anti-tumour activities against colon, prostate, breast and lung tumours [1–5]. These drugs are essential stimulants for the central nervous system that have the reputation of copycat psychoactive effects. Also, these classes of molecules are commonly used to produce some plastics, resins, pesticides, brake fluid and many other industrial materials for several important applications [6, 7]. The biological evaluation of piperazine derivatives has been investigated [8], but the physical assessment of N-(4-methoxyphenyl) piperazine isomers were not examined yet. One of the most important members of this class of molecules is N-(4-methoxyphenyl) piperazine (MeOPP). MeOPP has three isomers called as *ortho*-, *meta*- and *para*-MeOPP. Experimental and theoretical studies both have been carried out for various piperazine derivatives and reported in literature [9–12]. However, both experimental and theoretical studies on MeOPP molecule are quite insufficient for determination of the physical and chemical properties. The crystal structure of the *p*MeOPP molecule and its salts have been investigated recently [13]. A detailed theoretical and experimental study of the *o*MeOPP molecule was carried out by Prabavathi et al. [11]. In this study, FT-IR, FT-Raman, NMR and UV–Vis spectral measurements were experimentally investigated. Theoretically, the density functional theory (DFT) method, using B3LYP functional, with a 6-311++G (d, p) basis set, has been performed for assigning vibrational frequencies of *o*MeOPP molecule. In addition, molecular electrostatic potential (MEP) and natural bond orbital (NBO), highest occupied molecular orbital (HOMO), lowest unoccupied molecular orbital (LUMO) and nonlinear optical (NLO) properties have been studied. However, a literature search reveals that such a detailed study for *p*MeOPP and *m*MeOPP isomers has not been declared so far.

This study aims to obtain the most stable optimized structures of *p*MeOPP and *m*MeOPP isomers of molecules and to investigate the physical properties of these structures

✉ Hamdi Şükür Kılıç
hamdisukurkilic@selcuk.edu.tr

1 Faculty of Science, Department of Physics, Selçuk University, Konya 42031, Turkey

2 Directorate of High Technology Research and Application Center, Selçuk University, Konya 42031, Turkey

3 Directorate of Laser Induced Proton Therapy Application and Research Center, Selçuk University, Konya 42031, Turkey

4 Faculty of Ahmet Keleşoğlu, Department of Physics, Konya Necmettin Erbakan University, Konya 42090, Turkey

theoretically. To the best of the authors' knowledge, a detailed description of the physical properties of these isomers of molecule has been reported using neither experimental nor theoretical methods. It has also been shown how physical properties are affected for isomer structures.

2 Details of Calculation

In this work, firstly, conformer analysis for each isomer of MeOPP molecules was performed with the Spartan 08 package program [14], where conformational analysis was done using Merck molecular force field (MMFF) in the molecular mechanic method. Performance steps followed in the conformer analysis have been given in detail in previous studies [15, 16]. Secondly, a quantum chemical calculation for each isomer of MeOPP molecules was performed using the GAUSSIAN 09 program [17] with density functional theory [18] using the Becke three-parameter Lee–Yang–Parr exchange correlation functional (B3LYP) [19]. In addition, calculations were supplied by the standard 6-311++G (d,p) basis set. The UV–vis spectra of isomers have been computed by courtesy of time-dependent density functional theory (TD-DFT) [20] using the same basis set and exchange correlation functional.

3 Results and Discussion

3.1 Molecular Conformation and Geometrical Structure Analysis

Conformer analysis is an important step in obtaining the most stable structure of the molecule. Conformational analyses of *p*MeOPP, *m*MeOPP and *o*MeOPP isomers were carried out using the Spartan 08 package program with MMFF in the molecular mechanic method. As results of conformer analysis, *p*MeOPP, *m*MeOPP and *o*MeOPP compounds have one, two and five conformers, respectively. The shapes of these structures are shown in Fig. 1.

A calculation for geometry optimization is one of the most important steps in the theoretical studies. In order to determine stable conformations of isomers, structure and geometry optimizations of these conformers were performed using the B3LYP method with the 6-311++G(d,p) basis set and the most stable structures were determined. Also, the energy and dipole moments of the optimized structures are given in Table 1.

As shown in Table 1, the most stable structures of isomers are conf 1*p* of *p*MeOPP, conf 2*m* of *m*MeOPP and conf 5*o* of *o*MeOPP. Considering dipole moment values among isomers, it can be seen that they have an order of *o*MeOPP > *p*MeOPP > *m*MeOPP, from the largest one to the smallest one, respectively.

The selected geometric parameters (bond lengths, bond angles and dihedral angles) obtained from optimization calculations performed are presented in Table 2. The structural database analysis results specifically show the C–O–C–C dihedral angle which is usually 0° or 180°. The O–C–C angle at the aromatic ring is 115° or 125°. In the study, the O–C–C angle of isomers has been calculated as *p*MeOPP (116.2°), *m*MeOPP (124.1°) and *o*MeOPP (121.2°) respectively, in addition, the C–O–C–C dihedral angle of isomers has been calculated as *p*MeOPP (−0.29° or 179.7°) and *m*MeOPP (178.9°). However, this angle of the *o*MeOPP isomer is −77.06° and nearly orthogonal to the ring system. In addition, the methoxyphenyl group orientation in isomer structures was obtained as either co-planar with the aromatic ring or oriented nearly orthogonal to this ring system.

In literature, piperazines have been found generally in chair, half chair, boat, twist, boat and envelope forms [21, 22]. In this study, isomer structures of the MeOPP molecule have been obtained as chair conformation and approved by dihedral angles C1-N19-C5-C6. The *p*MeOPP isomer of the subject molecule has been experimentally studied; X-ray diffraction (XRD) data can be obtained [13] from literature, but XRD data for *m*MeOPP and *o*MeOPP isomers are not available yet in literature. Data from the *o*MeOPP isomer obtained by theoretical studies is also available and obtained from literature. By courtesy of these data, it can be concluded that our results obtained in this present work about molecular structures determined by conformer analysis are quite compatible with theoretical and experimental XRD results from literature.

3.2 HOMO–LUMO and Chemical Reactivity Descriptors

The main orbitals of a molecule are frontier molecular orbitals that are symbolized as highest occupied molecular orbital (HOMO) and lowest unoccupied molecular orbital (LUMO). HOMO symbolizes the stability to donate an electron of a molecular system, while LUMO symbolizes the stability to obtain an electron. The energy difference between HOMO and LUMO is known as the energy gap. It is an important parameter to assign electrical transport properties of a molecule and a measure of electron conductivity. Also, global chemical reactivity descriptors such as ionization potential (I), electron affinities (A), chemical potential (μ), absolute hardness (η), absolute softness (S), electrophilic index (ω) and electronegativity (χ) of a molecular system have been calculated by using HOMO and LUMO energies. All isomeric structures of high occupied orbital and low unoccupied orbitals of MeOPP molecule are shown in Fig. 2.

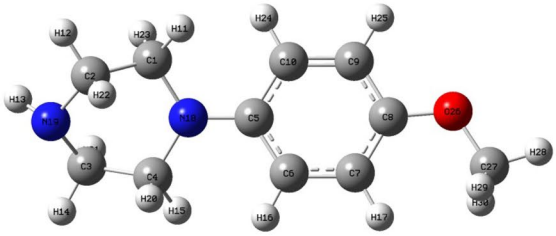

Conf 1*p*

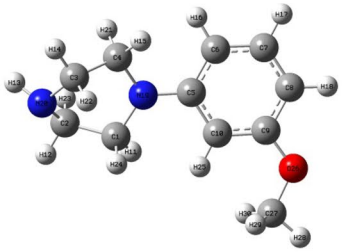

Conf 1*m*

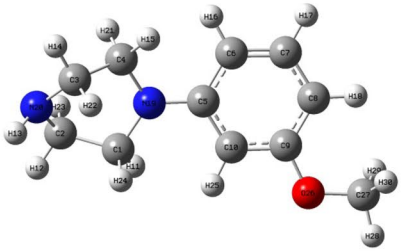

Conf 2*m*

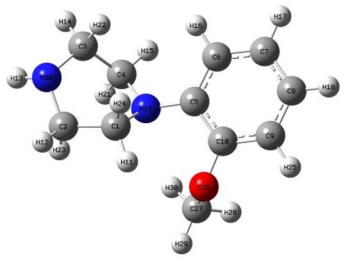

Conf 1*o*

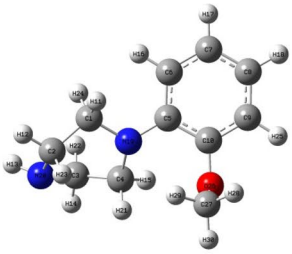

Conf 2*o*

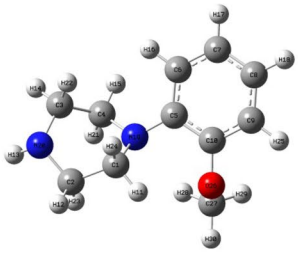

Conf 3*o*

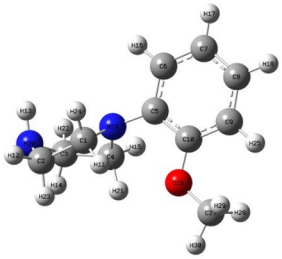

Conf 4*o*

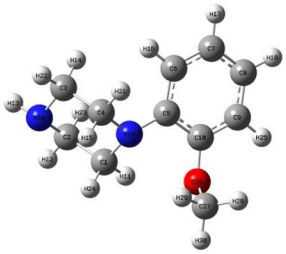

Conf 5*o*

Fig. 1 Possible conformers of *p*MeOPP, *m*MeOPP and *o*MeOPP isomers

Table 1 Conformer energies and dipole moment values of *p*MeOPP, *m*MeOPP and *o*MeOPP isomers

Piparazine isomers	Energies (Hartree)	Dipole moment (Debye)
Conf 1*p*	−613.660279	1.254798
Conf 1*m*	−613.663605	2.619863
Conf 2*m*	−613.664308	0.878440
Conf 1*o*	−613.651386	2.307071
Conf 2*o*	−613.654748	1.806450
Conf 3*o*	−613.651386	2.308061
Conf 4*o*	−613.655165	2.699673
Conf 5*o*	−613.662068	1.349426

The red- and green-coloured orbitals in the molecule show positive and negative phases. The obtained results show that LUMO structures in isomers are generally on the benzene ring while HOMO structure is in almost the whole molecule.

The chemical reactivity descriptors have been calculated by courtesy of Koopman's theorem [23]. In this theorem, I and A are the ionization potential and electron affinity, respectively. Ionization potential has been determined from $I = -E_{\mathrm{HOMO}}$ and the electron affinity has been calculated from $A = -E_{\mathrm{LUMO}}$. The chemical hardness and softness have been calculated by using $\eta = \frac{1}{2}\left[E_{\mathrm{LUMO}} - E_{\mathrm{HOMO}}\right]$ and $\mathrm{S} = \frac{1}{2\eta}$, respectively. Electronegativity has been determined by using the $\chi = -\frac{1}{2}\left[E_{\mathrm{HOMO}} + E_{\mathrm{LUMO}}\right]\chi = -\frac{1}{2}\left[E_{\mathrm{HOMO}} + E_{\mathrm{LUMO}}\right]$ formula [24]. The electrophilicity index has been determined by using the $\omega = \frac{\mu^2}{2\eta}$ formula [25]. The obtained chemical reactivity descriptors are given in Table 3.

The results obtained in this work indicate that the oMeOPP isomer is harder than other isomers and the *p*MeOPP isomer is softer than other isomers. The ionization potentials for *o*MeOPP, *m*MeOPP, and *p*MeOPP are 8.43, 8.32 and 7.94 eV, respectively. The electrochemical potential (μ) is in order of *m*MeOPP ≈ *p*MeOPP > *o*MeOPP. The electrophilicity values for isomers are in order of *p*MeOPP > *o*MeOPP ≈

Table 2 The selected geometric parameters of *p*MeOPP, *m*MeOPP and *o*MeOPP isomers

Parameters	*p*MeOPP-XRD [13]	*p*MeOPP	*m*MeOPP	*o*MeOPP
Bond lengths (Å)				
N19-C1	1.460 (3)[a]	1.46242	1.46031	1.47386
C1-C2	1.502 (4)[a]	1.53275	1.53162	1.53108
C2-N20	1.451 (4)	1.46866	1.46981	1.46581
N20-C3	1.435 (4)	1.47206	1.47084	1.46486
C3-C4	1.501 (4)	1.52667	1.52726	1.53509
C4-N19	1.457 (3)	1.45764	1.46138	1.46398
N19-C5	1.411 (3)	1.39272	1.38518	1.40736
C5-C10	1.395 (3)	1.41297	1.40561	1.41866
O26-C27	1.415 (4)	1.41701	1.41974	1.43276
C10-C9	1.378 (4)	1.38587	1.39627	1.39012
C9-C8	1.375 (3)	1.39767	1.39660	1.39355
C8-C7	1.380 (4)	1.39282	1.39658	1.39086
C7-C6	1.372 (4)	1.39759	1.38596	1.39305
C6-C5	1.389 (3)	1.40482	1.41619	1.40693
C9-O26	-	-	1.36936	-
C8-O26	1.375 (3)	1.37390	-	-
C10-O26	-	-	-	1.38364
Bond angle (◦)				
C3-C4-N19	110.71 (18)	110.44152	110.62893	113.21649
N20-C3-C4	109.6 (2)	110.93899	110.90171	108.63505
C2-N20-C3	109.6 (2)	113.86553	113.76687	111.59011
C1-C2-N20	109.9 (2)	113.89527	113.87800	109.30296
N19-C1-C2	110.8 (2)	109.85425	109.61380	111.47386
C4-N19-C1	111.8 (2)	116.96205	116.95513	111.20933
C4-N19-C5	115.72 (15)	120.95603	121.67421	120.17315
C6-C5-N19	120.58 (19)	122.05000	121.25852	122.97181
C5-C6-C7	122.5 (2)	121.61640	120.09389	121.90051
C6-C7-C8	119.9 (2)	120.47269	122.17351	120.46280

Table 2 (continued)

Parameters	*p*MeOPP-XRD [13]	*p*MeOPP	*m*MeOPP	*o*MeOPP
C7-C8-C9	118.8 (2)	118.65604	117.85848	118.78130
C8-C9- C10	121.2 (2)	120.93133	120.97437	121.07085
C5-C10-C9	120.9 (2)	121.39650	121.05061	121.05589
C10-C5-C6	116.7 (2)	116.92329	117.84712	116.64521
C10-C9-O26	-	-	114.89354	31.06477
C8-C9-O26	116.8 (2)	116.22106	124.12907	-
C9-O26-C27	-	-	118.45671	-
C5-C10-O26	-	-	-	121.22210
C10-O26-C27	-	-	-	114.55701
C7-C8-O26	124.4 (2)	27.23508	-	-
C8-O26-C27	117.7 (2)	118.08071	-	-
Dihedral angle (◦)				
N19-C4-C3-N20	−57.4 (3)	−61.64942	−61.31907	54.89936
C4-C3-N20-C2	61.8 (3)	28.29042	30.60912	−58.76103
C3-N20-C2-C1	−61.6 (3)	28.99314	26.91029	60.50631
N20-C2-C1-N19	57.0 (3)	−56.34969	−57.20875	−56.82031
C2-C1-N19-C4	−53.1 (3)	22.12055	25.66422	53.27165
C3-C4-N19-C1	53.5 (2)	33.69212	30.29170	−52.86897
C5-C6-C7-C8	0.1 (3)	0.64881	0.41301	0.95736
C6-C7-C8-C9	0.5 (3)	−0.36763	−0.08535	−1.78766
C7-C8-C9-C10	−0.1 (3)	−0.19971	−0.31536	0.08542
C8-C9-C10-C5	−0.8 (3)	0.50605	0.39035	2.48752
C9-C10-C5-C6	1.3 (3)	−0.23061	−0.06011	−3.21512
C10-C5-C6-C7	−1.0 (3)	−0.34172	−0.33245	1.52110
C1-N19-C5-C6	−174.17 (19)	157.91183	166.63178	128.14986
C27-O26-C10-C5	-	-	-	–77.06781
H30-C27-O26-C10	-	-	-	179.10091
H29-C27-O26-C10	-	-	-	59.65152
H28-C27-O26-C10	-	-	-	–62.27212
C27-O26-C8-C7	6.6 (4)	−0.29550	-	-
C27-O26-C8-C6	−173.1 (3)	179.75969	-	-
O26-C8-C7-C6	−179.1 (2)	179.68879	-	-
H30-C27-O26-C8	-	61.34753	-	-
H29-C27-O26-C8	-	−61.10778	-	-
H28-C27-O26-C8	-	−179.87889	-	-
C27-O26-C9-C10	-	-	−178.99620	-
H30-C27-O26-C9	-	-	60.90748	-
H29-C27-O26-C9	-	-	−61.58868	-
H28-C27-O26-C9	-	-	179.66983	-

[a]Estimated standard deviations refer to the last decimal place [13]

*m*MeOPP, while the electronegativity values are ranked as *o*MeOPP > *m*MeOPP > *p*MeOPP.

3.3 Nonlinear Optical Properties

The nonlinear optical properties (NLO) of the MeOPP isomer were studied by calculating the dipole moment, the polarizability and the first hyper polarizability using the B3LYP/6-311++G(d,p) level of DFT theory. The dipole moment (μ), the polarizability (α) and the first hyper polarizability (β) have been calculated from the equations given below and are reported in Table 4.

The total dipole moment (μ_{tot}) for the molecule is defined as in Eq. 1:

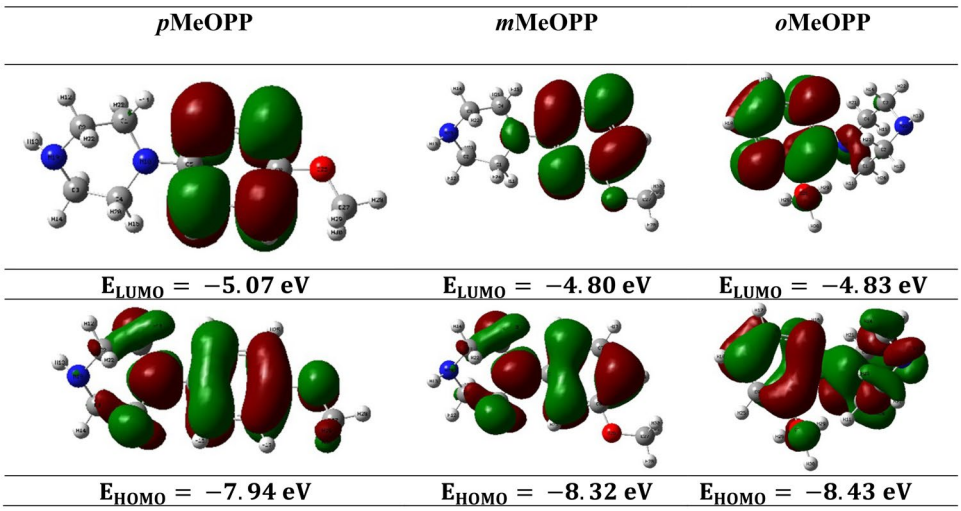

Fig. 2 HOMO and LUMO for *p*MeOPP, *m*MeOPP and *o*MeOPP isomers

$$\mu_{\text{tot}} = \left(\mu_x + \mu_y + \mu_z\right)^{1/2} \tag{1}$$

Total polarizability (α_{tot}) for the molecule can be evaluated as in Eq. 2:

$$\alpha_{\text{tot}} = \frac{1}{3}\left(\alpha_{xx} + \alpha_{yy} + \alpha_{zz}\right) \tag{2}$$

The total first hyper polarizability (β_{tot}) can be calculated as in Eq. 3:

$$\beta_{\text{tot}} = \left(\beta_x^2 + \beta_y^2 + \beta_z^2\right)^{1/2} \tag{3}$$

were β_x, β_y and β_z are defined to be

$$\beta_x = \left(\beta_{xxx} + \beta_{xyy} + \beta_{xzz}\right) \tag{4}$$

$$\beta_y = \left(\beta_{yyy} + \beta_{yzz} + \beta_{yxx}\right) \tag{5}$$

$$\beta_z = \left(\beta_{zzz} + \beta_{zxx} + \beta_{zyy}\right) \tag{6}$$

The total first hyper-polarizability from the Gaussian 09 output is given in Eq. 7.

$$\beta_{\text{tot}} = \left[\left(\beta_{xxx} + \beta_{xyy} + \beta_{xzz}\right)^2 + \left(\beta_{yyy} + \beta_{yzz} + \beta_{yxx}\right)^2 + \left(\beta_{zzz} + \beta_{zxx} + \beta_{zyy}\right)^2\right]^{1/2} \tag{7}$$

The dipole moment is one of some important results for electronic properties due to the distribution of charges on atoms in a molecule and used to investigate the intermolecular interactions. The higher the dipole moment is, the stronger the intermolecular interactions are. The polarizability and the first hyper-polarizability characterize the response of a molecule in an applied electric field [26]. (The calculated β_{tot} and α_{tot} values in Table 4 were converted into electrostatic units (esu) [1 a.u. = 8.6393×10^{-33} esu] and [1 a.u. = 0.1482×10^{-24} esu], respectively [27, 28].) As seen in Table 4, the polarizability values of the *p*MeOPP, *m*MeOPP and *o*MeOPP isomers have been calculated to be 23.099×10^{-24}, 23.056×10^{-24} and 22.391×10^{-24}, respectively. Also, the first hyper-polarizability values of *p*MeOPP, *m*MeOPP and *o*MeOPP isomers have been obtained as 1121.59×10^{-33}, 3943.84×10^{-33} and 3869.82×10^{-33}, respectively. It has been noticed that some very good NLO properties have arisen due to two nitrogen atoms in the structure of isomers [29]. From the obtained results, these isomers are an appealing molecule for future studies of NLO applications.

3.4 Mulliken Population Analysis

Atomic charge calculation has been carried out to show the distribution of positive and negative charges in molecules. This calculation is important to examine some increases or decreases in bond lengths between atoms. Atomic charges can affect many molecular properties such as dipole moment, polarizability and

Table 3 Chemical reactivity descriptors of *p*MeOPP, *m*MeOPP and *o*MeOPP isomers

Isomers	E_{gap} (eV)	I (eV)	A (eV)	μ (eV)	η (eV)	S (eV)	ω (eV)	χ (eV)
*p*MeOPP	2.87	7.94	5.07	−6.50	1.43	0.34	14.77	6.50
*m*MeOPP	3.52	8.32	4.80	−6.56	1.76	0.28	12.22	6.56
*o*MeOPP	3.6	8.43	4.83	−6.63	1.8	0.27	12.21	6.63

Table 4 The values of calculated dipole moment (μ), polarizability (α), first-order hyper-polarizability (β) components of *p*MeOPP, *m*MeOPP and *o*MeOPP isomers

Parameters	*p*MeOPP	*m*MeOPP	*o*MeOPP
Dipole moment (Debye)			
μ_x	−1.0419	−0.2048	−1.0635
μ_y	−0.5806	−0.3960	−0.6766
μ_z	−0.3897	0.7569	−0.4818
μ_{tot}	1.2548	0.8784	1.3494
Polarizability (a.u)			
α_{xx}	218.400	212.449	181.778
α_{yy}	144.162	149.806	158.435
α_{zz}	105.034	104.472	113.062
α_{tot}(a.u)	155.865	155.575	151.092
α_{tot} (esu)	23.099×10^{-24}	23.056×10^{-24}	22.391×10^{-24}
Hyper-polarizability (a.u)			
β_{xxx}	123.956	474.358	316.372
β_{xxy}	−7.045	270.795	−180.236
β_{xyy}	111.148	−204.184	51.262
β_{yyy}	−37.590	−6.992	−39.850
β_{xxz}	42.760	−55.731	−5.427
β_{xyz}	69.567	73.561	−40.646
β_{yyz}	−7.676	39.992	−34.062
β_{xzz}	−14.241	52.522	1.757
β_{yzz}	−53.072	57.787	−21.275
β_{zzz}	50.388	−13.245	−37.566
β_{tot} (a.u)	129.825	456.501	447.933
β_{tot}(esu)	1121.59×10^{-33}	3943.84×10^{-33}	3869.82×10^{-33}
Parameters	*o*MeOPP	*m*MeOPP	*p*MeOPP
Dipole moment (Debye)			
μ_x	−1.0635	−0.2048	−1.0419
μ_y	−0.6766	−0.3960	−0.5806
μ_z	−0.4818	0.7569	−0.3897
μ_{tot}	1.3494	0.8784	1.2548
Polarizability (a.u)			
α_{xx}	181.778	212.449	218.400
α_{yy}	158.435	149.806	144.162
α_{zz}	113.062	104.472	105.034
α_{tot}(a.u)	151.092	155.575	155.865
α_{tot}(esu)	22.391×10^{-24}	23.056×10^{-24}	23.099×10^{-24}
Hyper-polarizability (a.u)			
β_{xxx}	316.372	474.358	123.956
β_{xxy}	−180.236	270.795	−7.045
β_{xyy}	51.262	−204.184	111.148
β_{yyy}	−39.850	−6.992	−37.590
β_{xxz}	−5.427	−55.731	42.760
β_{xyz}	−40.646	73.561	69.567
β_{yyz}	−34.062	39.992	−7.676
β_{xzz}	1.757	52.522	−14.241
β_{yzz}	−21.275	57.787	−53.072
β_{zzz}	−37.566	−13.245	50.388
β_{tot}(a.u)	447.933	456.501	129.825
β_{tot}(esu)	3869.82×10^{-33}	3943.84×10^{-33}	1121.59×10^{-33}

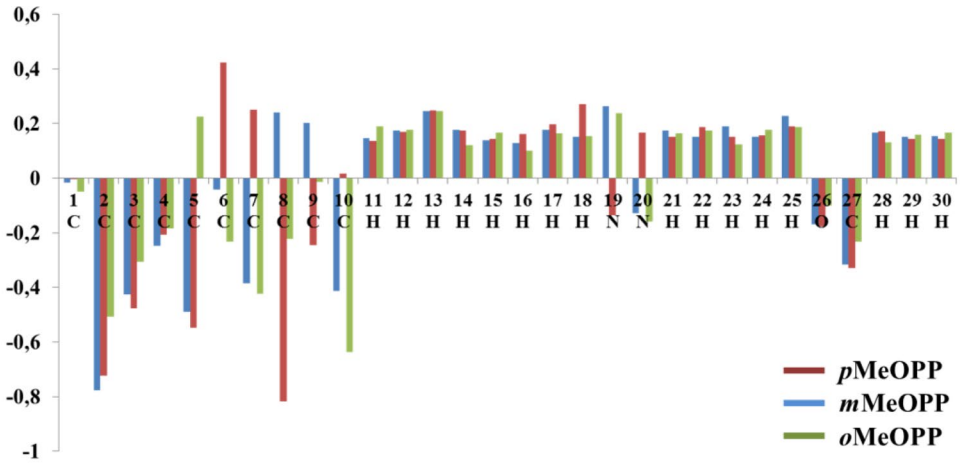

Fig. 3 Mulliken population for *p*MeOPP, *m*MeOPP and *o*MeOPP isomers

electronic structure. Total atomic charges of Mulliken population analysis are given in Fig. 3.

According to Mulliken population analysis, although the *o*MeOPP isomer has a positive charge for C5, *m*MeOPP and *p*MeOPP isomers have negative charges for C5. This situation for the *m*MeOPP isomer has a positive charge for C8 and C9; they have negative charges for other isomers. In addition, the *p*MeOPP isomer has a positive charge for C6 and C7 while they have negative charges for other isomers. Another important point is that the *p*MeOPP isomer has a positive charge distribution at N20 while other isomers have a negative charge distribution. The *p*MeOPP isomer has a negative charge distribution at N19 while other isomers have a positive charge distribution.

3.5 Molecular Electrostatic Potential Map

The MEP map can be used to distinguish regions where the surface is electron rich or poor. The red and yellow colours on the MEP map correspond to negative electrostatic potential regions and the blue colour corresponds to the positive electrostatic potential region. In addition, it can be employed to investigate the relationship between the molecular structure and physiochemical properties of molecules including biomolecules and drugs (Fig. 4) [30–34].

The colour codes of these MEP maps are in the range between -7.981×10^{-2} a.u and 7.981×10^{-2} a.u and -7.429×10^{-2} a.u and 7.429×10^{-2} a.u and -6.865×10^{-2} a.u

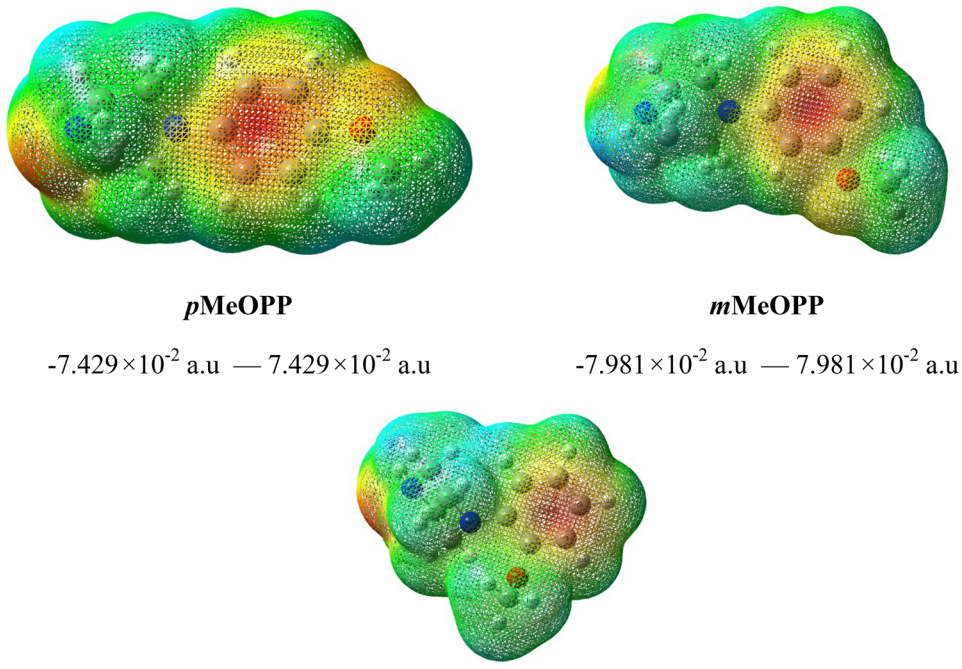

Fig. 4 MEP map diagram for *p*MeOPP, *m*MeOPP, and *o*MeOPP isomers

Table 5 The thermodynamic parameters for *p*MeOPP, *m*MeOPP and *o*MeOPP isomers

	*p*MeOPP	*m*MeOPP	*o*MeOPP
Total energy (thermal), *E* total (kcal mol−1)			
Total	170.785	170.845	170.866
Electronic	0.000	0.000	0.000
Translational	0.889	0.889	0.889
Rotational	0.889	0.889	0.889
Vibrational	169.008	169.067	169.088
Heat capacity at const. volume, C v (cal. mol−1 K−1)			
Total	50.531	50.574	49.875
Electronic	0.000	0.000	0.000
Translational	2.981	2.981	2.981
Rotational	2.981	2.981	2.981
Vibrational	44.570	44.613	43.914
Entropy, *S* (cal. mol−1 K−1)			
Total	115.211	114.723	110.597
Electronic	0.000	0.000	0.000
Translational	41.664	41.664	41.664
Rotational	31.806	31.915	31.533
Vibrational	41.741	41.144	37.400
Zero-point vibrational energy, E 0 (kcal mol−1)	162.53701	162.60885	162.94986
Rotational constants (GHz)			
A	2.38073	1.72244	1.09703
B	0.29423	0.33729	0.53945
C	0.27058	0.29244	0.42170

and 6.865×10^{-2} a.u. *m*MeOPP, *p*MeOPP and *o*MeOPP respectively. In addition, the obtained results show that the negative potential of nitrogen due to the red colour is presented, but the positive potential is shown at hydrogen atoms.

3.6 Thermodynamic Properties

The thermodynamic parameters of the isomer are shown in Table 5. The thermodynamic results obtained can make useful data for further experimental studies on MeOPP isomers, when these were used to investigate the interaction between MeOPP molecule and another molecule [35]. According to thermodynamic results obtained, total energy (thermal) values of isomers varied in only vibrational levels and these values have been obtained in an order of *o*MeOPP > *m*MeOPP > *p*MeOPP from largest to smallest. Heat capacity values are varied at the same level as thermal values. However, the order of heat capacity among isomers has

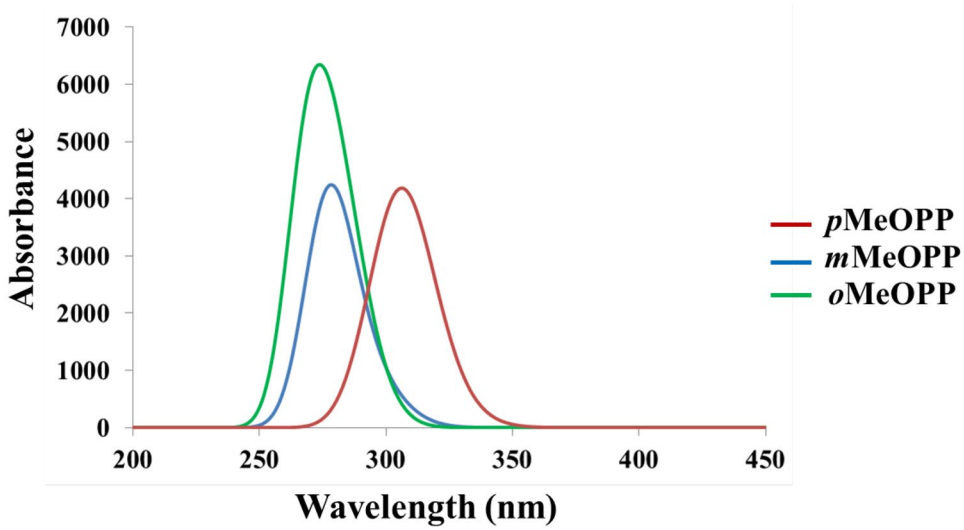

Fig. 5 UV–Vis spectrum for *p*MeOPP, *m*MeOPP and *o*MeOPP isomers

Table 6 Absorption wavelengths, electronic excitation energies, oscillator strength, and major contributions values for *p*MeOPP, *m*MeOPP and *o*MeOPP isomers

İsomers	Excited state	Calculated values			
		Excitation energies (eV)	Wavelength (nm) (λ)	Oscillate strengths (*f*)	Major contributions
*p*MeOPP	S_1	3.86	320.88	0.0032	HOMO→LUMO (96%)
	S_2	4.03	306.99	0.0501	HOMO→L+1 (95%) H-2→L+6 (2%)
	S_3	4.20	294.56	0.0103	HOMO→L+2 (96%)
*m*MeOPP	S_1	4.17	296.61	0.0079	HOMO→LUMO (96%)
	S_2	4.45	278.40	0.0501	HOMO→L+1 (43%) HOMO→L+2 (46%) H-1→L+5 (2%) H-1→L+7 (3%)
	S_3	4.56	271.73	0.0085	HOMO→L+1 (48%) HOMO→L+2 (35%) HOMO→L+3 (12%)
*o*MeOPP	S_1	4.35	285.01	0.0297	HOMO→LUMO (72%) HOMO→L+1 (22%) H-2→L+2 (3%)
	S_2	4.48	276.64	0.0234	HOMO→LUMO (24%) HOMO→L+1 (71%)
	S_3	4.61	268.84	0.0568	HOMO→L+2 (90%) HOMO→L+4 (5%)

been changed as *m*MeOPP > *p*MeOPP > *o*MeOPP from largest to smallest, whereas the entropy values have shown some differences in both rotational and vibrational levels and, due to these differences, they were ordered from largest to smallest to be *p*MeOPP > *m*MeOPP > *o*MeOPP.

3.7 UV–Vis Spectral Analysis

UV–vis spectral analysis of MeOPP isomers has been calculated theoretically. TD-DFT is an important tool used to investigate the static and dynamic properties of any molecule in their exited states [20]. Graphs of data obtained were plotted by GaussSum [36]. The computed absorption bands were obtained for mMeOPP isomers at 296.61 nm, 278.40 nm and 271.73 nm; for *o*MeOPP isomers at 285.01 nm, 276.64 nm and 268.84 nm; and for *p*MeOPP isomers at 320.88 nm, 306.99 nm and 294.56 nm. As a result, the absorption wavelength varies for each isomer. However, as seen clearly in Fig. 5, it is prominently different for *p*MeOPP isomers. In addition, for *p*MeOPP isomers, the absorption band is found at 275 nm in literature [37]. This difference is due to that theoretical calculations were carried out in gas phase while experimental work was in solution.

Calculated absorption wavelengths, electronic excitation energies, oscillator strength and major contribution values for MeOPP isomers are represented in Table 6. Major contributions for isomers have been observed in HOMO→LUMO with (96%) in 296.61 nm for *m*MeOPP isomers, in HOMO→L+2 with (90%) in 268.84 nm for *o*MeOPP isomers and HOMO→LUMO with (96%) in 320.88 and HOMO→L+2 with (96%) in 294.56 nm for *p* MeOPP isomers.

4 Conclusion

In this study, the optimized geometrical parameters, HOMO and LUMO energies, chemical reactivity descriptors, nonlinear optical properties, Mulliken population analysis, molecular electrostatic potential map, thermodynamic properties and UV–Vis spectral analysis of MeOPP isomers have been investigated using DFT and TD-DFT/B3LYP/6-311++G(d,p) method and represented in present work. Structural properties of *p*MeOPP isomer gathered from XRD analysis in literature have been found to be quite compatible. In addition, in general, results of the bond length, for example, between C–C atoms obtained for other isomers in literature have also been found to be compatible. The band gap values change as in the order of *o*MeOPP > *m*MeOPP > *p*MeOPP according to HOMO and LUMO results obtained for isomers and chemical reactivity descriptors were obtained from these values. MeOPP isomers show some significant dipole moments, polarizability and hyper-polarizability, so these isomers show some good NLO properties; this is due to two nitrogen atoms in the structure of isomers. According to Mulliken results, it can be said that the *p*MeOPP isomer is found to be different from other isomers. Thermodynamic data provides quite good information for experimental studies on MeOPP isomers. Absorption bands of the *p*MeOPP isomer as a result of UV–Vis analysis have been observed at 320.88 nm, 306.99 nm and 294.56 nm. In addition, under the scope of obtained theoretical data, we hope that this study will be a guiding study for both experimental and theoretical studies to understand structural isomers for the physics, chemistry and pharmaceutical industries.

Acknowledgements The authors kindly would like to thank Selçuk University, Faculty of Science, Department of Physics, Selçuk University, High Technology Research and Application Center for supplying Infrastructure and SULTAN Center.

References

1. L.K. Basco, J.A.C.Q.U.E.S. Le Bras, Antimicrob. Age. Chemother. **36**(1), 209–213 (1992)
2. A.M. Oduola, A. Sowunmi, W.K. Milhous, T.G. Brewer, D.E. Kyle, L. Gerena, B.G. Schuster, Am. J. Trop. Med. Hyg. **58**(5), 625–629 (1998)
3. A.J. Bitonti, A. Sjoerdsma, P.P. McCann, D.E. Kyle, A.M. Oduola, R.N. Rossan, D.E. Davidson, Science **242**(4883), 1301–1303 (1988)
4. A.F. Coutaux, J.J. Mooney, D.F. Wirth, Am. J. Trop. Med. Hyg. **38**(6), 1419–1421 (1994)
5. A. Varga, H. Nugel, R. Baehr, U. Marx, A. Hevér, J. Nacsa, J. Molnar, Anticancer Res. **16**(1), 209–211 (1996)
6. P. Molander, K. Haugland, G. Fladseth, E. Lundanes, S. Thorud, Y. Thomassen, T. Greibrokk, J. Chromatogr. A. **892**(1–2), 67–74 (2000)
7. G. Moghadam, F. Tirgir, A.H. Reshak, M. Khorshidi, Mater. Chem. Phys. **236**, 121780 (2019)
8. K. R. Varadaraju, J. R. Kumar, L. Mallesha, A. Muruli, K. N. S. Mohana, C. K. Mukunda, U. Sharanaiah, Int. J. Alzh. Disease. 2013 (2013)
9. Y.S. Mary, C.Y. Panicker, C.N. Kavitha, H.S. Yathirajan, M.S. Siddegowda, S.M. Cruz, J.A. War, Spectrochim. Acta A Mol. Biomol. Spectrosc. **137**, 547–559 (2015)
10. G. Keşan, Ö. Bağlayan, C. Parlak, Ö. Alver, M. Şenyel, Spectrochim. Acta A Mol. Biomol. Spectrosc. **88**, 144–155 (2012)
11. N. Prabavathi, N. Senthil Nayaki, N. V. Krishnakumar, Pharm. Anal. Acta. **6**(391), 2 (2015)
12. G. Dikmen, .A. Ü. Bilm. Tekn. Derg. **20**(2), 133–142 (2019)
13. H. Kiran Kumar, H. S. Yathirajan, C. Harish Chinthal, S. Foro, C. Glidewell, Acta. Cryst. E. **76**(4), 488–495 (2020)
14. Y. Shao, L.F. Molnar, Y. Jung, J. Kussmann, C. Ochsenfeld, S.T. Brown, Jr. R.A. DiStasio, Phys. Chem. Chem. Phys. **8**, 3172–3191 (2006)
15. Ö. Dereli, Opt. spectrosc. **120**(5), 690–700 (2016)
16. Y. Ekincioğlu, H.Ş Kılıç, Ö. Dereli, J. Selcuk-Technic. **3**, 199–208 (2016)
17. M. Frisch, G.W. Trucks, H.B. Schlegel, G.E. Scuseria, M.A. Robb, J.R. Cheeseman, H. Nakatsuji, Wallingford CT. (2009)
18. P. Hohenberg, W.J.P.R. Kohn, Phys. Rev. **136**, B864 (1964)
19. C. Lee, W. Yang, R.G. Parr, Phys. Rev. B. **37**(2), 785 (1988)
20. R. Improta, V. Barone, J. Am. Chem. Soc. **126**(44), 14320–14321 (2004)
21. J.B. Hendrickson, J. Am. Chem. Soc. **83**(22), 4537–4547 (1961)
22. R.G. Lett, L. Petrakis, A.F. Ellis, R.K. Jensen, J. Phys. Chem. **74**(14), 2816–2822 (1970)
23. T. Koopmans, Physica. **1**(1–6), 104–113 (1934)
24. L. Pauling, The Nature of the Chemical Bond, (Cornell university press Ithaca, 1960), pp. 3175–3187
25. R.G. Parr, L.V. Szentpaly, J. Am. Chem. Soc. **121**(9), 1922–1924 (1999)
26. A. D. Buckingham, Adv. Chem. Phys. 107–142 (1967)
27. P.N. Prasad, D.J. Williams, *Introduction to Nonlinear Optical Effects in Molecules and Polymers* (Wiley, New York, 1991)
28. I.C. de Silva, R.M. de Silva, K.N. De Silva, J. Mol. Strc. **728**(1–3), 141–145 (2005)
29. K. Subashini, S. Periandy, J. Mol. Struct. **1134**, 157–170 (2017)
30. O. Prasad, L. Sinha, N. Kumar, J. At. Mol. Sci. **1**, 201–214 (2010)
31. I. Alkorta, J.J. Perez, Int. J. Quan. Chem. **57**(1), 123–135 (1996)
32. B.H. Lengsfield, D.R. Yarkony, Adv. Chem. Phys. **82**(2), 1–71 (1992)
33. J. S. Murray, K. Sen, Molecular electrostatic potentials, (Elsevier, 1996)
34. P. Politzer, J.S. Murray, Murray. Theor. Chem. Acc. **108**(3), 134–142 (2002)
35. R. Zhang, B. Du, G. Sun, Y. Sun, Spectrochim. Acta A Mol. Biomol. Spectrosc. **75**(3), 1115–1124 (2010)
36. N.M. O'Boyle, J.G. Vos, GaussSum 1.0. (Dublin City University, 2005)
37. U. Geiger, Y. Haas, J. Phys. Chem. B. **119**(24), 7338–7348 (2015)